

$m = 2, k = +5$ gives for $a^{-1} - 1 < \epsilon < 1$ a highly interesting family of solutions passing close to E and M , with no exceptional ϵ values in this range. Solution curves passing near E and M can also be generated, starting from $\xi^* = a(1 - \epsilon)$ and η^* by [2], when $k - m$ is odd. The corresponding solutions $x^*(t)$ are obtained from the previous ones using [2] by rotation through $-\pi(1 - m/k) \cdot \text{sign } k$, but for $\mu > 0$ this relation will be distorted. Such solutions can be made to come close to M at a later time (not at apogee). The choice $m = 1, k = +2$ yields promising flight paths for solar probes returning to Earth after a little less than 1 yr.

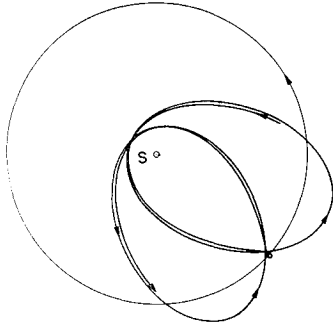


Fig. 3 Circular paths of E, M , and the path from Fig. 1 in inertial co-system nearly from $t = 0$ to $t = 2T$; capture and rejection of P by M

The perturbations encountered on actual flights, for which the restricted three-body problem is only an idealization, could be controlled essentially by employing continuous electric or other propulsions. Practical uses of certain of the periodic flight paths, whose existence has been established mathematically, can be conceived readily. This paper mentions only a radiation protected heavy Earth-moon ferry

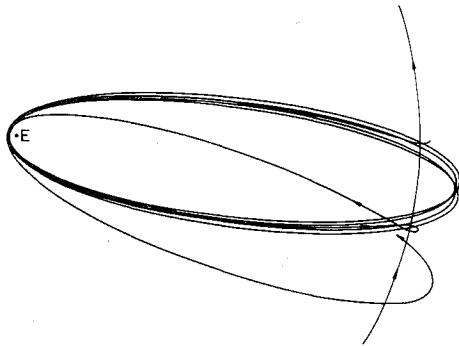


Fig. 4 Circular arc of M and the path from Fig. 2 as seen from E under space-fixed orientation from $t = 0$ to nearly $t = \frac{1}{2}T$; capture and rejection of P by M

vehicle perpetually on such a path, to be supplied or boarded by passengers after rendezvous with much smaller crafts near E or M , which themselves could return to their bases, for instance. This would relieve the necessity to launch a heavy space ship from Earth or to assemble it in Earth orbit for every new flight to the moon and landing back on Earth. Thus tourist trips to the moon and back become practical and more economical.

A few illustrations are included which are calculated for the case $\mu = \frac{1}{8}$. Figs. 1 and 2 show synodically closed solution curves of [1] for $m = 1, k = 2$ and $m = 2, k = 5$, respectively, in the rotating co-system. Fig. 3 shows for the first case the circular paths of E and M and the path of P in an inertial co-system with origin at S . Fig. 4 shows for the second case the paths of P and M in a co-system with origin at E and space-fixed orientation. Note the short time capture of P by M with subsequent rejection which happens after elapse of every T units of time, i.e., every time when P has completed nearly k Keplerian elliptic orbits with focus at E .

Radiation Environment Following a Nuclear Attack

R. A. PORTER¹ AND R. L. HATFIELD²

Martin Company, Denver, Colo.

This article describes an analytical model that can predict postblast nuclear radiation levels following an air burst of any size and proximity. It is also an attempt to assemble in one place all the salient subexpressions and considerations that must be incorporated into a computer program for complete prosecution of the model's details. The initial condition assumed is that an overhead nuclear detonation, sufficiently high to preclude significant fallout, has just occurred. An oblate, spheroid-shaped cloud is rising, growing, and emitting gamma rays at an ever-decreasing rate. The radiation dose rate at any discrete time i and altitude j is then calculated by the expression

$$\dot{D}_{ij} = \sum_{k=H_{bot}i}^{H_{top}i} \sum_{l=0}^{r_{0i}} \sum_{m=1}^4 1.602 \times 10^{-8} F_{im} \times \left(\frac{\mu_a}{\rho}\right)_m B_{ijklm} E_m S_{vi} \frac{\exp[-(\mu/\rho)_m \bar{r}_{ijkl} R_{ijkl}]}{4\pi(R_{ijkl})^2}$$

A sample case of a 20-MT burst is considered, and curves of dose rates vs altitudes at several discrete instants in time are generated.

THE effect that nuclear radiation may have on electronic devices is of crucial concern to designers of weapons systems. Several informative articles dealing with susceptibilities of components and circuits to radiation have appeared recently in unclassified literature (2,3),³ but to incorporate these considerations intelligently into his system concept, the designer also needs to know the greatest amount of radiation the system might receive.

It is, of course, impossible to predict numbers, sizes, and proximities of nuclear detonations that might occur in the event of attack. However, one can hypothesize an array of this sort and obtain radiation environment curves, which will enable the designer to make definitive statements concerning component selection, "hold" times, etc., required for successful missions immediately following a nuclear attack.

By definition, "... a typical air burst takes place at such a height that the fireball, even at its maximum, is well above the surface of the earth" (1).

Description of Analytical Model

The initial condition assumed is that an overhead nuclear detonation sufficiently high to preclude significant fallout has just occurred. An oblate spheroid-shaped cloud is rising, growing, and emitting gamma rays at an ever-decreasing rate. Also, the system, in this case a missile, has been protected from the burst's primary radiation pulse and peak air overpressure. Such would be the case for a hardened underground silo (4). It is desired to find radiation levels as functions of times and altitudes following this detonation.

Define the following:

- i = time after air burst, sec
- j = distances of a fictitious aboveground radiation "detector," cm. At each discrete time i chosen following the burst, this detector will be moved from one

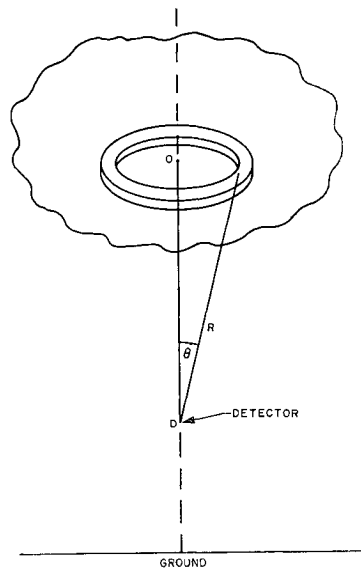
Received by ARS September 27, 1962.

¹ Design Specialist.

² Supervisor, Small Computers Unit.

³ Numbers in parentheses indicate References at end of paper.

Fig. 1 Pictorial representation of annual increment of radiating cloud that is a distance R from detector



- altitude to another, computing the dose rate that it will see at each discrete altitude (see Fig. 1)
- k = distance above ground of radiating cloud increment, cm. This will be the distance from the ground to the altitude of initial detonation plus the distance the cloud has risen from the burst point to the instant in time considered (see Fig. 1)
- l = horizontal displacement of annular cloud volume increment from vertical axis through the center of the cloud (see Fig. 1)
- m = average energy of gamma ray group (=0.125, 0.625, 1.35, 2.5 Mev; see Fig. 2)

The expression for the dose rate that the detector will see at any discrete time and altitude can now be written as

$$\dot{D}_{ij} = \sum_{k=H_{bot\ i}}^{H_{top\ i}} \sum_{l=0}^{r_{0i}} \sum_{m=1}^4 1.602 \times 10^{-8} F_{im} \times \left(\frac{\mu_a}{\rho}\right)_m B_{ijkl} E_m S_{vi} \frac{\exp[-(\mu/\rho)_m \bar{\rho}_{ijkl} R_{ijkl}]}{4\pi(R_{ijkl})^2}$$

where

- \dot{D}_{ij} = dose rate that the detector will see at time i , following the detonation and elevation j , rad/sec
- $H_{top\ i}$ = height of top of cloud from ground at time being considered. Normalizing Anderson's model (5) to Fig. 2.12 of Glasstone (1) will generate this as $H_{top} = H_{burst} + 1.89 \times 10^4 W^{0.25}/t^{0.50}$ cm, where W is the weapon yield in kilotons and t is the time from burst in seconds. The cloud top will reach its maximum altitude at $t_m = 510.3 - 33.9 \ln W$ sec
- $H_{bot\ i}$ = height of bottom of cloud from ground at time being considered. Normalizing Anderson's model to Fig. 2.12 of Glasstone generates this as $H_{bot} = H_{burst} + 8.53 \times 10^3 W^{0.25}/t^{0.50}$ cm. The cloud bottom will reach its maximum altitude at the same time as the top
- r_{0i} = horizontal (major) radius of oblate spheroid-shaped cloud at time being considered. This is given by Anderson as $r_0 = 1.66 \times 10^4 t^{0.25} \times W^{0.11}/t^{0.22}$ cm. The authors have also devised a separate expression to calculate the maximum radius that the cloud will achieve as shown in Fig. 2.16 of Glasstone (1). This will be $r_{max} = 1.22 \times 10^5 + 3.94 \times 10^4 e^{0.5 \ln W}$ cm

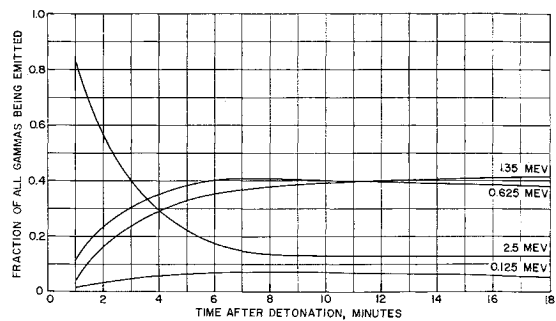


Fig. 2 Relative abundance of fission fragment gamma ray energy groups (adapted from calculations of Ref. 6)

- F_{im} = fraction of cloud's radioactivity that is assigned to the m th gamma ray energy group (see Fig. 2). The assigning of fission fragment gammas to each of these groups was accomplished by inspection of the data of Refs. 6 and 7
- $(\mu_a/\rho)_m$ = energy absorption mass attenuation coefficient in air for m th gamma ray energy group [=0.0242 cm²/g for 0.125 Mev, 0.0295 cm²/g for 0.625 Mev, 0.0263 cm²/g for 1.35 Mev, 0.0224 cm²/g for 2.5 Mev gammas (8)]
- B_{ijklm} = dosage buildup factor for air with point isotropic source (9)
 $= A_{1m} \exp[-\alpha_{1m}(\mu/\rho)_m \bar{\rho}_{ijkl} R_{ijkl}] + A_{2m} \times \exp[-\alpha_{2m}(\mu/\rho)_m \bar{\rho}_{ijkl} R_{ijkl}]$. This term accounts for the effect that scattered primary gammas of the m th energy group will have at the detector [see Table 1 for values of A and α ; values of $(\mu/\rho)_m$ are given below]
- \bar{E}_m = average energy of m th gamma ray group (0.125, 0.625, 1.35, 2.5 Mev)
- S_{vijkl} = total gamma ray inventory per unit cloud volume multiplied by increment of volume of cloud being considered. An adaptation (6) of the Way-Wigner formula (11) will generate this as $A = 1.46 \times 10^{23} W t^{-1.2}$ gammas/sec for a burst that is 100% fission
- $(\mu/\rho)_m$ = total mass attenuation coefficient in air for m th gamma ray energy group [=0.1425 cm²/g for 0.125 Mev, 0.079 cm²/g for 0.625 Mev, 0.0546 cm²/g for 1.35 Mev, 0.0401 cm²/g for 2.5 Mev gammas (8)]
- $\bar{\rho}_{ijkl}$ = average density of air between radiating cloud increment and detector. To facilitate computer calculations of air density as a function of altitude, the authors devised a separate analytical model to fit the NACA density curve (10)
- ρ = $0.98 \times 10^{-3} \exp(-\{0.813 + 0.783[1 - \exp(-[H - 1.83 \times 10^6 \text{ cm}]/[1.92 \times 10^{-6} \text{ cm}])\}10^{-6}H)$, where H is height of cloud

Table 1 Values of A and α for calculating dose buildup factor B in air (adapted from Ref. 5)

Average energy of m th gamma ray group, meV	A_2		α_1	α_2
	A_1	$(=1 - A_1)$		
0.125	35.3	-34.9	-0.220	0
0.625	20.0	-19.5	-0.125	0
1.35	8.4	-7.9	-0.092	0.065
2.5	5.7	-5.2	-0.067	0.101

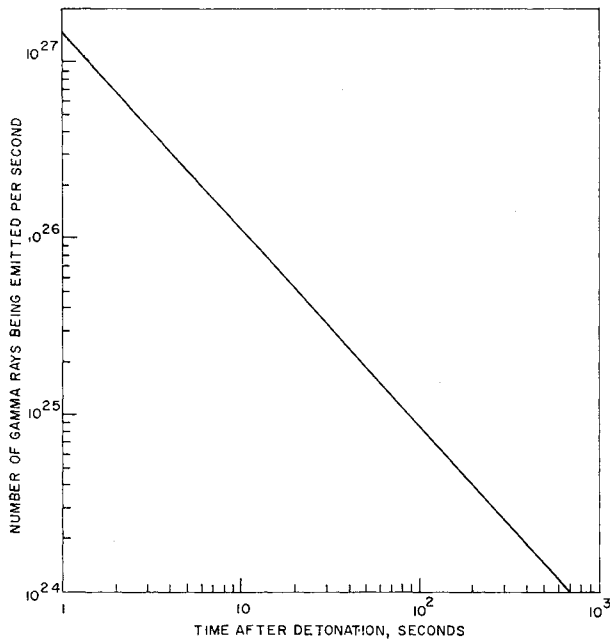


Fig. 3 Total gamma ray inventory in radioactive cloud following detonation of 20-MT weapon (assumes 50% of energy due to fission; adapted from Ref. 11)

increment above sea level in centimeters, and R_{ijkl} is distance in centimeters from detector to cloud increment (see Fig. 1)

The factor 1.602×10^{-8} in the foregoing equation results from the fact that 1 rad is defined as 100 erg/g of radiation energy dissipated in any irradiated material and that 1 Mev = 1.602×10^{-6} erg.

Results and Discussion

Fig. 3 shows a typical result obtained using the analytical model. In this case, a 20-MT weapon, half of whose energy yield was due to fission, was detonated 7000 ft above ground. The elevation at ground level was taken as 6000 ft above sea level. No prevailing winds were assumed. The annular widths and heights (Fig. 1) were assigned a value of 100 m.

The effect that variation in air density has on the amount of radiation seen by the detector is quite apparent, as evidenced by the asymmetry of dose rate above and below the cloud center at $T + 4$ min.

Fig. 4 was generated, using the Bendix G-15 computer, in approximately 3.5 hr of computing and readout time. More

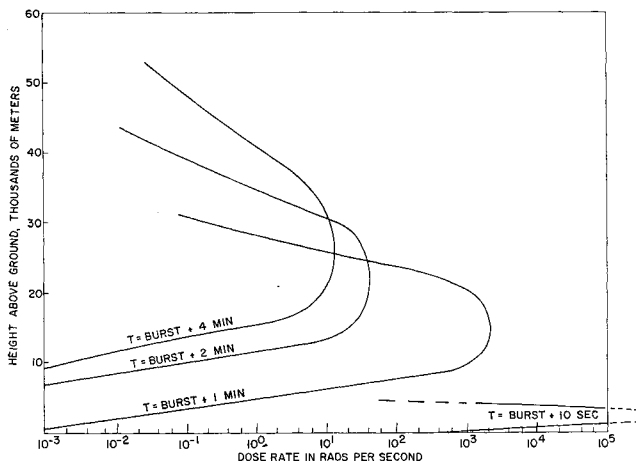


Fig. 4 Radiation dosage at discrete times and elevations following a 20-MT air burst ($H_{burst} = \text{ground} = 7000$ ft; $\text{ground} = 6000$ ft above sea level)

accurate results could be obtained using a faster computer, dividing the cloud's volume into smaller annuli.

References

- 1 Glasstone, S. (ed.), *The Effects of Nuclear Weapons* (U. S. Government Printing Office, Washington, D. C., 1962), pp. 10, 34, 36, 689.
- 2 Kaplan, A. L., "Investigating radiation effects on electronic devices," *Aerospace Eng.* 21, 40-50 (July 1962).
- 3 Clarke, J. W. and Hanscome, T. D., "Radiation pulses and electronics," *Nucleonics* 18, 74-78 (September 1960).
- 4 Kudroff, M. J., "The first Titan hardened facilities," *Aerospace Eng.* 20, 10-12 (June 1961).
- 5 Anderson, A. D., "The NRDL dynamic model for fallout from land-surface nuclear bursts," U. S. Navy Research Dev. Lab. TR-41D (April 5, 1960), pp. 22, 32.
- 6 Kerr, T. B. and Walton, R. B., "Results obtained using an IBM 704 program for computing U^{235} fission-product populations, activities, and powers," Air Force Special Weapons Center Rept. TN-59-19 (August 1959).
- 7 Gamble, R. L., "Prompt fission gamma rays from uranium 235," doctoral dissertation, Univ. Texas, Austin, Texas (June 1955).
- 8 Blizard, E. P., "Nuclear radiation shielding," *Nuclear Engineering Handbook*, edited by H. Etherington (McGraw-Hill Book Co. Inc., New York, 1958), 1st ed., pp. 7-62.
- 9 Rockwell T., III, *Reactor Shielding Design Manual* (McGraw-Hill Book Co. Inc., New York, August 1959), p. 420.
- 10 "Pocket data for rocket designers," Bell Aircraft Corp. (June 1958).
- 11 Way, K. and Wigner, E. P., "The rate of decay of fission products," *Phys. Rev.* 73, 1318 (1948).

Solar Cell Performance in the Artificial Radiation Belt

ROBERT E. FISHELL*

The Johns Hopkins University, Applied Physics Laboratory, Silver Spring, Md.

As a result of the high altitude nuclear test performed over Johnston Island on July 9, 1962, an intense electron radiation belt has been created. The electrons in this artificial belt have a sufficiently high energy and density to impair seriously the operation of solar cell power generating systems. Special solar cell panels on the Transit 4B and TRAAC satellites have shown a 22% decrease in output in a period of approximately 25 days after the high altitude nuclear test. Using solar cell data obtained from Transit 4B and TRAAC in conjunction with direct radiation measurements from other satellites, it is possible to estimate the degradation of solar power generating systems for various satellite orbits.

Introduction

THE Transit 4B and TRAAC satellites were launched into the same orbit from Cape Canaveral, Fla., on November 15, 1961. The Transit 4B and TRAAC satellites each contained experiments to determine the performance of solar cells in the space environment. Over a period of 236 days, from launch until July 9, 1962, performance of these solar cells indicated a damage rate that was consistent with present knowledge of the proton flux levels of the inner Van Allen radiation belt. As a result of the high altitude nuclear weapon test of July 9, 1962, the radiation at altitudes of great interest for earth satellites was changed vastly as to both its character and its intensity. As a result of the explosion, a high flux rate of energetic electrons (in the energy region above 100 kev) was more or less permanently trapped at altitudes from as low as 200 miles to as high as 12,000 miles and possibly beyond.

Design of the Solar Cell Experiments

For monitoring the performance of solar cells in the space environment, the Transit 4B satellite employed a single solar

Presented at the ARS Space Power Systems Conference, Santa Monica, Calif., September 25-28, 1962.

* Project Supervisor, Space Power Systems. Member ARS.